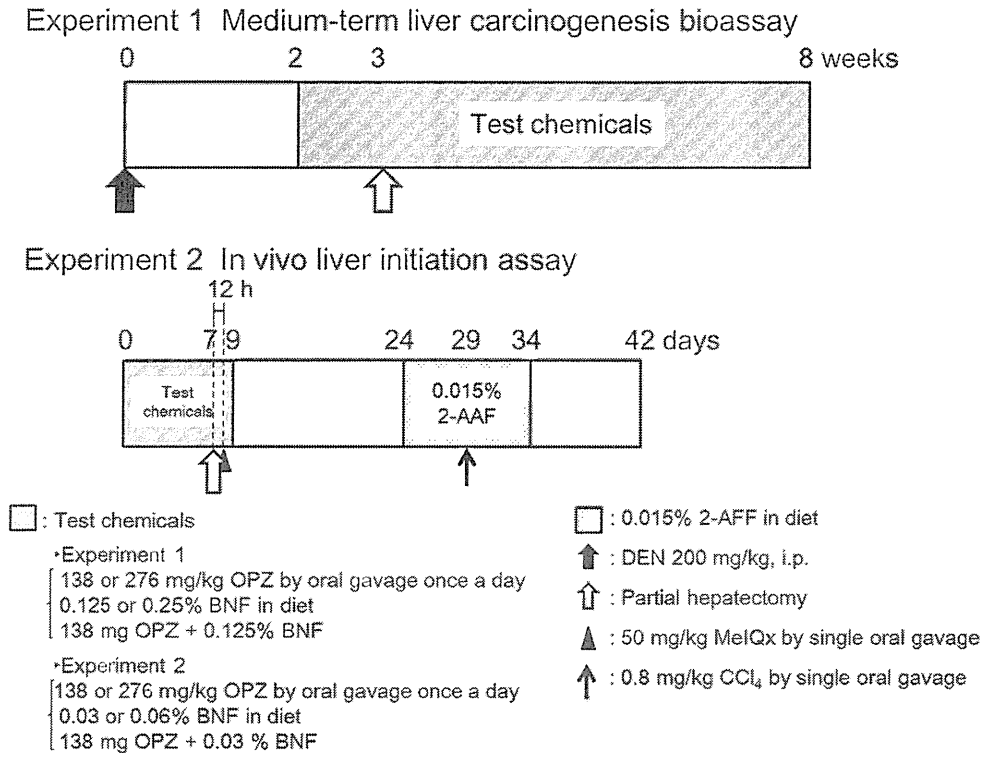

Fig. 1. Experimental design of a medium-term liver carcinogenesis bioassay (Experiment 1) and an *in vivo* liver initiation assay (Experiment 2) in rats.

Experiment 2

An *in vivo* 5-week liver initiation assay was performed according to the method described by Tsuda *et al.* (1980). To examine the modification of MeIQx-induced liver tumor initiating effect by co-administration of BNF and OPZ, we modified the duration of this *in vivo* liver initiation assay to 6 weeks. The experimental design is shown in Fig. 1. First, all rats were treated with 0 (MeIQx alone), 138 mg/kg OPZ (Low OPZ) or 276 mg/kg OPZ (High OPZ) by oral gavage once a day, 0.03% BNF (Low BNF) or 0.06% BNF (High BNF), or 138 mg/kg OPZ + 0.03% BNF (OPZ+BNF) for 9 days starting 1 week before initiating treatment. The rationale for the dosage was determined based on the results from our previous studies in which 0.06% BNF induced *Cyp1a1* and *Cyp1a2* expression, being approximately 1923-fold and 8-fold higher than those of the DEN control, and 276 mg/kg OPZ induced *Cyp1a1* and *Cyp1a2* expression, being approximately 1163-fold and 9-fold higher than those of the DEN control group (Hayashi *et al.*, 2012a, 2012b). As an initiation treatment, 50 mg/kg MeIQx was orally administered 12 hr after PH. One day after the initiation, the rats were fed a basal diet for 15 days, followed by a diet containing 0.015% 2-AAF for 10 days to enhance the tumor-promoting effect. Also, to damage their livers, they were orally administered CCl_4 (0.8 ml/kg bw) dissolved in corn oil on day 29. At the end of the experiment, the rats were euthanized by exsanguination under ether anesthesia and their livers were excised and weighed. The sliced liver samples were fixed in 10% phosphate-buffered formalin for histopathological and immunohistochemical examination.

Histopathology and immunohistochemistry

After formalin fixation of the livers in Experiments 1 and 2, the tissues were dehydrated in graded ethanol and embedded in paraffin. Sections were then mounted onto glass slides and were stained with hematoxylin and eosin or were used for immunohistochemistry analysis. For immunohistochemistry, the horseradish peroxidase avidin-biotin complex method with a Vectastain Elite ABC

kit (Vector Laboratories Burlingame, CA, USA) was used. Endogenous peroxidase was inhibited by incubation with freshly prepared 0.3% hydrogen peroxide with methanol for 30 min. The sections were incubated overnight with rabbit polyclonal anti-glutathione *S*-transferase placental form (GST-P) antibody (Medical & Biological Laboratories, Nagoya, Japan; 1:1,000), mouse monoclonal anti-proliferative cell nuclear antigen (PCNA) antibody (DAKO, Glostrup, Denmark; 1:800) and mouse monoclonal anti-cyclooxygenase-2 (COX-2) antibody (BD Biosciences, Tokyo, Japan; 1:250, Experiment 1 only) at 4°C, followed by incubation with a biotinylated secondary antibody for 30 min and with avidin peroxidase conjugate for 30 min at room temperature. The sections were then developed in 0.05% 3, 3'-diaminobenzidine/hydrogen peroxide as the chromogen. For PCNA staining and COX-2 staining, the deparaffinized tissue sections were placed in an antigen-retrieval solution (0.01 M citrate buffer, pH 6.0) for 20 min in a hot bath at 60°C or autoclaved at 121°C for 10 min prior to immunohistochemical staining. After staining, the slides were lightly counterstained with hematoxylin.

The numbers and areas of GST-P-positive foci (≥ 0.2 mm in diameter) and total areas of the liver sections were quantified using WinRoof software (v5.7.2; Mitani Corp., Fukui, Japan). The number of PCNA-positive cells and COX-2-positive cells counted under × 200 magnification, was expressed as a percentage of the total cells or area counted in 20 randomly selected fields (including foci). In both analyses, cranial and caudal parts of the right lateral liver lobe were used.

Definition of zones in the liver

Suzuki *et al.* (2010) showed that the intralobular difference of GST-P-positive foci expression is related to the MeIQx-hepatocarcinogenesis. Therefore, for the determination of intralobular differences of GST-P-positive foci expression in the liver of Experiment 2, we defined the GST-P-positive foci adjacent to Glisson's sheath as zone 1, adjacent to the central vein as zone 3, and adjacent to both Glisson's sheath and the central vein, or not adjacent to either of them, as zone 2, using the method described by Suzuki *et al.* (2010).

cDNA microarray analysis

Total RNA of the liver obtained from Experiment 1 was extracted with an RNeasy Mini Kit (QIAGEN, Hilden, Germany), in accordance with the manufacturer's instructions. Using 10 μg of total RNA from one animal from each of the controls, 138 mg/kg OPZ, 0.125% BNF and 138 mg/kg OPZ+0.125% BNF groups, double-stranded cDNA was synthesized with an Invitrogen Superscript Double-Stranded cDNA Synthesis kit (Invitrogen Corp., CA, USA), in accordance with the manufacturer's protocol. After labeling with Cy3, 6 μg of each of the Cy3-labeled cDNA sample were loaded onto a *Rattus norvegicus* Roche NimbleGen Microarray for Gene Expression (Roche NimbleGen: Euk Expr 385K catalog Arr, 26,739 targets/microarray). Using the robust multiple average normalization method (Irizarry *et al.*, 2003), differentially expressed genes were analyzed. Gene information was retrieved from the National Center for Biotechnology Information website (http://www.ncbi.nlm.nih.gov).

Real-time RT-PCR analysis

Total RNA of the liver obtained from Experiment 1 was extracted with an RNeasy Mini Kit (QIAGEN), in accordance with the manufacturer's instructions. Reverse transcription was carried out with 2 μg RNA for cDNA synthesis using a Thermoscript RT-PCR System kit (Eppendorf Co., Ltd., Tokyo, Japan), in accordance with the manufacturer's protocol. Quantitative real-time RT-PCR with Power SYBR Green PCR Master Mix (Applied Biosystems Japan Ltd., Tokyo, Japan) was performed using a StepOnePlus™ Real-time PCR System (Applied Biosystems Japan Ltd.). The PCR primers (listed in Table 1) were designed using Primer Express software (Version 3.0; Applied Biosystems Japan Ltd.). The amount of target gene expression was normalized to an endogenous reference (actin, beta) and relative to a control was obtained using the $2^{-\Delta\Delta Ct}$ method (Livak and Schmittgen, 2001).

Lipid peroxidation levels

Oxidative lipid peroxidation was estimated using TBARS. Hepatic TBARS levels were determined using the method described by Ohkawa *et al.* (1979) with a slight modification. The liver tissue samples (approximately 50 mg) obtained from Experiment 1 were homogenized in 450 μl of buffer (containing 50 mM Tris-HCl; pH7.4, 1.15% KCl, 0.2 mM EDTA, 0.1 mM dithiothreitol (DTT), 0.1 mM Protease Inhibitor Cocktail and 20% glycerol) using TissueLyser (QIAGEN). Aliquots of 3 mg of liver homogenates were mixed with 0.2 ml of 8.1% sodium dodecyl sulfate and 3 ml of 0.4% thiobarbituric acid in 10% acetic acid (pH 3.5), heated at 95°C for 60 min and then cooled. Each reaction mixture was centrifuged at 4,000 rpm for 10 min after adding 1 ml of distilled water and 5 ml of n-butanol and pyridine (15:1, v/v). The absorbance of the resulting solution was determined spectrophotometrically at 532 nm, using a Synergy HT Multi-Detection Microplate Reader (BioTek, Winooski, VT, USA). The TBARS levels were expressed as the equiva-

Table 1. Primers used for real-time RT-PCR

Accession no.	Gene description	Symbol	Forward primer	Reverse primer
NM_012540	Cytochrome P450, family 1, subfamily am polypeptide 1	*Cyp1a1*	gccttcacatcagccacaga	ttgtgactctaaccacccagaatc
NM_012541	Cytochrome P450, family 1, subfamily am polypeptide 2	*Cyp1a2*	aagcgccggtgcattg	tgcaggaggatggctaagaag
NM_012940	Cytochrome P450, family 1, subfamily b, polypeptide 1	*Cyp1b1*	cttggccattgatcggaaa	caaggcgagcgaagtacaaagt
NM_001198676	Cytochrome P450, family 2, subfamily b, polypeptide 2	*Cyp2b2*	gggacactgaaaaagagtgaagct	aatgccttcgccaagacaaat
NM_022407	Aldehyde dehydrogenase 1 family, member A1	*Aldh1a1*	agtgccccttcggtggat	gctcagtgtactcataaagaccatgttc
NM_031972	Aldehyde dehydrogenase 3 family, member A1	*Aldh3a1*	tggagcctcatcctggcttat	gaatttggaggagtgaggtgaga
NM_017000	NAD(P)H dehydrogenase, quinone 1	*Nqo1*	tccgcccccaacttctg	tctgcgtgggccaataca
NM_001039691	UDP glucuronosyltransferase 1 family, polypeptide A6	*Ugt1a6*	tggctaccccaaaacgatct	ataccatgggaaccggagtgt
NM_001024285	Aryl-hydrocarbon receptor repressor	*Ahrr*	gctgctggagtctctcaatgg	gcccaggtagtccacaattgtt
NM_013215	Aldo-keto reductase family 7, member A3	*Akr7a3*	ccgcttctttgggaatccat	ggcgatgccattgaagtgt
NM_183403	Glutathione peroxidase 2	*Gpx2*	accgatcccaagctcatcat	tctcaaagttccaggacacatctg
NM_001159739	Glutathione S-transferase Yc2 subunit	*Yc2*	aagctgagcagggctgatgt	acaatgcctgggtccatctc
NM_012600.2	Malic enzyme 1, NADP(+)-dependent, cytosolic	*Me1*	cgaccagcaaagctgagtgtt	ctgccgctggcaaagatc
NM_017232	Cyclooxygenase-2	*Cox-2*	ttcgacttttccaggatggaa	gagtgtctttgactgtgggaggat
NM_012620	Serpin peptidase inhibitor, clade E , member 1	*Serpine1*	tggctcagaacaacaagttcaac	ggcagttccaggatgtcgtact
NM_053963	Matrix metallopeptidase 12	*Mmp12*	gcgaggctgacattacgatactt	taaggtaccacctttgccatca
NM_012589	Interleukin 6	*Il6*	cccaccaggaacgaaagtca	cttgcggagagaaacttcatagc
NM_130752	Fibroblast growth factor 21	*Fgf21*	gccaacaaccagatggaactc	tccttaagcagcagctctctga
XM_342346	Nuclear factor of kappa light polypeptide gene enhancer in B-cells 1	*Nfkb1*	gaagtacagaggaaacgcaccagaag	ccgccgccgaaactg
NM_001105720	Rattus norvegicus nuclear factor of kappa light polypeptide gene enhancer in B-cells inhibitor, alpha	*Nfkbia*	gcctagccccgagcattc	aatgatctgtttccccaaatttca
NM_012675	Tumor necrosis factor	*Tnf*	acaaggctgccccgactat	ctcctggtatgaagtggcaaatc
NM_053677	Checkpoint kinase 1	*Chek1*	tggcagctggcaaagga	aatcccagtcttccacaaaagg
NM_001012742	Wee 1 homolog (S. pombe)	*Wee1*	cggcaaactcctcaagtgaatatt	cactgtcctgaggaatgaagcat
NM_012603	Myelocytomatosis oncogene	*Myc*	cgcctctgggaaactttgc	tcctggctcgcagattgtaa
NM_031144	Actin, beta	*Actb*	ccctggctcctagcaccat	agagccaccaatccacacaga

lents of malondialdehyde (MDA) amounts that were produced from 1,1,3,3,-tetramethoxypropane.

Preparation of microsomal fraction

The microsomal fractions were obtained according to the methods described by Yoshihara *et al.* (2001). Liver tissue samples (approximately 100 to 130 mg) obtained from Experiment 2 were homogenized in 700 μl of ice-cold buffer (containing 50 mM Tris-HCl; pH 7.4, 1.15% KCl, 0.2 mM ethylene diamine tetra-acetic acid, 0.1 mM DTT, 0.1 mM Protease Inhibitor Cocktail and 20% glycerol) using a pestle. The homogenate was centrifuged at 700 × g for 10 min at 4°C, and the supernatant was centrifuged at 10,000 × g for 20 min at 4°C. The 500 μl of supernatant was ultracentrifuged at 105,000 × g for 90 min. The microsomal pellet was resuspended in microsome buffer, and the protein content of the homogenate was measured using the BCA Protein Assay Kit (Pierce, IL, USA), with bovine serum albumin as a standard.

Microsomal reactive oxygen species production

NADPH-dependent microsomal ROS production was determined by measuring the oxidation of 2',7'-dichlorodihydrofluorescein diacetate (H_2DCFDA) to its fluorescent product 2',7'-dichlorofluorescein in liver microsomes according to the methods described by Schlezinger *et al.* (1999). The microsomes (final concentration 0.2 mg/ml) obtained from Experiment 1 were incubated in the dark at 37°C for 30 min in 50 mM Tris-HCl (pH 7.4) and 5 μM H_2DCFDA. In addition, 2.5 mM β-NADPH was

added. In some cases, 0.1 mM SKF-525A (Toronto Research Chemicals, ON, Canada), a well-known inhibitor of CYP, and 0.1 mM H_2O_2 as a positive control were added to the wells. The fluorescence was monitored every 5 minutes over 2 hr using a Synergy HT Multi-Detection Microplate Reader (BioTek) with excitation and emission wavelengths of 485 and 528 nm, respectively. The data were then normalized to the control values, with the control expressed as a value of 100%.

Plasma concentration of OPZ and BNF

To measure the plasma concentration of OPZ and BNF, the HPLC system (Waters chromatography division, Milford, MA, USA) was used in Experiment 1. Blood samples were collected from three rats each in the High OPZ, High BNF and OPZ+BNF groups. The blood sampling was performed one hour after administration of OPZ during the morning time. Chromatographic separation of OPZ or BNF was achieved using a Cadenza CD-C18 (3 μm, 4.6 mm I.D. × 150 mm, Imtakt) reverse phase analytical column. The mobile phase consisted of a mixture of 10 mmol/l phosphate buffer/acetonitrile (13:7, v/v adjusted pH to 7.3 with triethylamine) or a mixture of acetonitrile/25 mmol/l potassium dihydrogen phosphate (7:3, v/v). The mobile phase was pumped at an isocratic flow rate of 1.3 ml/min at 40°C or 1.5 ml/min at 40°C. The wavelength of UV detection was set at 302 and 285 nm for OPZ and internal standard solution (IS) (Lansoprazole: LPZ) assays, respectively or 274 nm for BNF and IS (hexyl 4-hydroxybenzoate) assays.

Plasma samples were collected at an hour after a final oral dose of OPZ. Plasma samples (400 μl) were transferred to a 15 ml glass tube, and 160 μl of diluent, 10 mmol/l disodium hydrogen phosphate for the OPZ assay, or a mixture of water/acetonitrile (1:1, v/v) for the BNF assay, was added. Then 40 μl of IS working solution (5 μg/ml) was spiked. A 2 ml aliquot of extraction solvent, tert-butyl methyl ether, was added and the sample was shaken for 10 min before being centrifuged for 3 min at 3,000 rpm. The organic layer (1.5 ml) was quantitatively transferred to a 6 ml glass tube and evaporated under a stream of nitrogen. The dried extract was then reconstituted with 200 μl of mobile phase, and a 20 μl aliquot was injected into chromatographic system.

For calibration samples, to 400 μl of blank rat plasma, 160 μl of working standard of OPZ or BNF was added, yielding final concentrations of 20-2,000 ng/ml of OPZ and BNF. To this mixture, 40 μl of IS working solution was added to yield IS concentration of 500 ng/ml.

Statistical analysis

All data were expressed as mean with standard deviation. Numerical data were evaluated using the following methods: A Bartlett's test for equal variance was used to determine if the variance was homogenous between the groups. If the variance was homogenous, numerical data were assessed using Dunnett's multiple comparison test. If a significant difference in variance was observed, the Steel test was used instead. In addition, to estimate the modifying effect of the combined administration, statistical analysis was performed using the method recommended by Futakuchi *et al.* (1996) and Hasegawa *et al.* (1991).

RESULTS

Experiment 1

Body and liver weights, food intake and BNF intake

In all treated groups, body weight significantly decreased when compared with the DEN alone group (Table 2). In the OPZ+BNF group, body weight significantly decreased when compared with other treated groups.

The absolute and relative liver weights significantly increased in the treated groups when compared with the DEN alone group. The relative liver weight in the OPZ+BNF group was approximately 1.8-fold higher than that in the DEN alone group, and was significantly higher than the High OPZ or High BNF groups (Table 2).

Food intake did not fluctuate with the treatment of OPZ or BNF, and average BNF intakes were 0.08 ± 0.01, 0.17 ± 0.01 and 0.09 ± 0.01 g/kg body weight/day in the Low BNF, High BNF and OPZ+BNF groups, respectively. The food efficiency in the DEN alone group, Low/High OPZ, Low/High BNF and OPZ+BNF groups was 0.17, 0.15, 0.15, 0.19, 0.16 and 0.11, respectively. A decreasing tendency of food efficiency was observed in the Low/High OPZ, High BNF and OPZ+BNF groups when compared to the DEN alone group.

Histopathology, GST-P-positive foci and PCNA-positive cells in the liver

Histopathologically, both OPZ and BNF induced diffuse hepatocellular hypertrophy with eosinophilic cytoplasm. Foci of cellular alterations of clear cells, eosinophilic cells and basophilic cells were observed in the treated groups. There was no inflammatory change in the OPZ, BNF and OPZ+BNF groups. Immunohistochemical analysis revealed that the number/area of GST-P-positive foci significantly increased in the treated groups (Table 2, Figs. 2a and b). In the OPZ+BNF group, the number of

Table 2. Final body and liver weights, food intake, BNF intake, number/area of GST-P-positive foci, PCNA-positive cells, ROS production and TBARS in the liver of male F344 rats given OPZ and/or BNF for 6 weeks after DEN treatment

Final body weight (g)	DEN alone	Low OPZ	High OPZ	Low BNF	High BNF	OPZ+BNF
No. of animals	11	12	12	9	12	11
Final body weight (g)	278.13 ± 9.65	258.86 ± 11.93**,##	255.59 ± 14.83**,##	267.62 ± 11.69##	260.68 ± 14.79**,##	233.01 ± 14.97**
Absolute liver weight (g)	8.25 ± 0.40	9.32 ± 0.67**,##	10.17 ± 0.84**,##	10.44 ± 0.91**,#	11.23 ± 0.89**	11.98 ± 1.40**
Relative liver weight (g/100 g body weight)	2.97 ± 0.10	3.60 ± 0.22**,##	3.97 ± 0.15**,##	3.90 ± 0.22**,##	4.30 ± 0.18**,##	5.14 ± 0.53**
Average food intake (g/kg body weight/day)	14.81 ± 1.12	14.48 ± 1.20	13.81 ± 1.10	14.11 ± 1.43	14.17 ± 1.58	13.50 ± 2.04
Average BNF intake (g/kg body weight/day)	-	-	-	0.08 ± 0.01	0.17 ± 0.01	0.09 ± 0.01
GST-P positive foci (≧ 0.2 mm)						
Numbers (number/cm²)	3.18 ± 1.93	4.47 ± 1.65##	5.78 ± 2.18*,##	7.05 ± 1.45**,##	7.30 ± 2.45**,##	10.66 ± 2.76**
Areas (mm²/cm²)	0.20 ± 0.12	0.37 ± 0.27##	0.42 ± 0.20*,##	0.57 ± 0.20**	0.58 ± 0.31**	0.82 ± 0.34**
PCNA-positive cells (%)	0.29 ± 0.18	0.25 ± 0.19#	0.41 ± 0.18	0.36 ± 0.18	0.39 ± 0.22	0.64 ± 0.41*
No. of animals	5	5	5	5	5	5
ROS production (%)						
+NADPH	100.00 ± 16.72	75.19 ± 5.91**	71.77 ± 10.81**	91.12 ± 6.52	76.22 ± 15.32**	68.32 ± 7.55**
+NADPH+SKF525A	48.55 ± 7.32	42.74 ± 5.43	45.23 ± 8.35	43.77 ± 5.24	47.25 ± 6.76	43.17 ± 4.94
-NADPH	21.36 ± 2.54	21.36 ± 1.10	21.24 ± 1.08	21.91 ± 2.05	17.00 ± 9.59	20.96 ± 3.14
No. of animals	6	6	6	6	6	6
TBARS (nmol MDA/mg protein)	0.97 ± 0.08	0.99 ± 0.06	1.00 ± 0.05	1.00 ± 0.04	1.01 ± 0.12	0.93 ± 0.07

DEN, *N*-diethylnitrosamine; Low OPZ, 138 mg/kg omeprazole; High OPZ, 276 mg/kg omeprazole; Low BNF, 0.125% β-naphthoflavone; High BNF, 0.25% β-naphthoflavone; and OPZ+BNF, 138 mg/kg omeprazole + 0.125% β-naphthoflavone. The data represent mean ± S.D.

*, ** significantly different from the DEN alone group at $P < 0.05$ or 0.01.

#, ## significantly different from the OPZ +BNF group at $P < 0.05$ or 0.01.

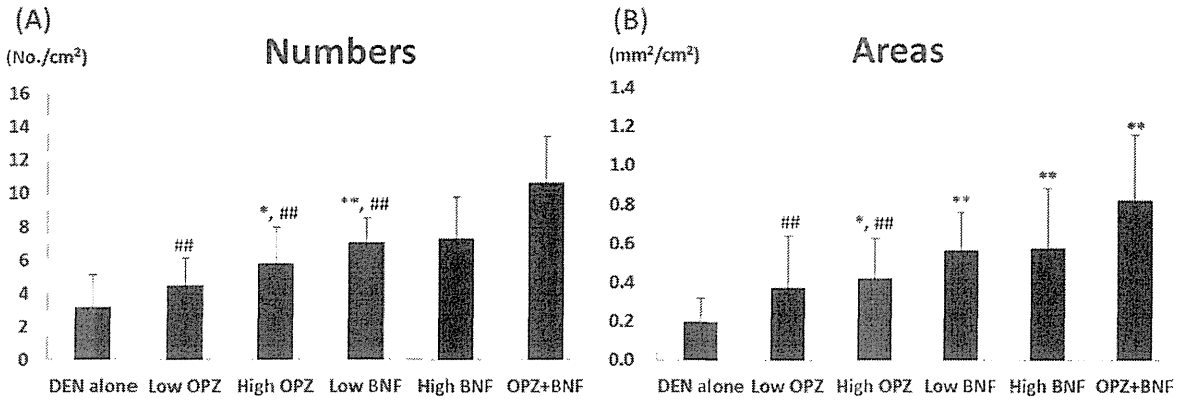

Fig. 2. Number and area of GST-P-positive foci in rats given OPZ and/or BNF after DEN initiation. Each bar shows the number (A) and area (B) of GST-P-positive foci in the liver of rats given DEN alone (DEN alone), 138 mg/kg OPZ (Low OPZ), 276 mg/kg OPZ (High OPZ), 0.125% BNF (Low BNF), 0.25% BNF (High BNF) or 138 mg/kg OPZ+0.125% BNF (OPZ+BNF). *, ** significantly different from the DEN alone group at $P < 0.05$ or $P < 0.01$, respectively. ## significantly different from the OPZ+BNF group at $P < 0.01$.

GST-P-positive foci significantly increased when compared with the OPZ treated and BNF treated groups, and the area of GST-P-positive foci significantly increased when compared with the OPZ treated groups. Meanwhile, the number of PCNA-positive cells significantly increased in the OPZ+BNF groups when compared with the DEN alone group (Table 2).

DNA microarray and real-time RT-PCR analyses

Hepatic gene expression changes in rats from the DEN alone, Low OPZ, Low BNF and OPZ+BNF groups were screened using an oligonucleotide microarray. In the microarray, 4,439 genes showed more than a 2-fold increase or more than a half-fold decrease in their expression in one rat each from the OPZ, BNF and OPZ+BNF groups when compared with a rat of the DEN alone group (supplementary data). We focused on the AhR battery and oxidative stress response-related genes. Real-time RT-PCR analysis on the genes listed in Table 1 was performed using liver samples (6 rats/group) (Table 3).

In real-time RT-PCR analysis, the expression of *Cyp1a1*, *Cyp1a2*, *Cyp1b1*, *Ugt1a6* and *Nqo1*, which are phase I metabolic enzymes and are regulated by AhR, significantly increased in the treated groups when compared with the DEN alone group. Of these genes, the expression of *Cyp1a2*, *Cyp1b1*, *Ugt1a6* and *Nqo1* significantly increased in the OPZ+BNF group when compared with the Low OPZ or Low BNF groups (Table 3). The expression of *Aldh1a1* and *Cyp2b2* significantly increased in the OPZ treated groups, but showed a decreasing tendency in the OPZ+BNF group when compared with the OPZ treated group. On the other hand, *Aldh3a1* significantly increased in the BNF treated groups when compared with the DEN alone group, and significantly increased in the OPZ+BNF group when compared with the Low OPZ or Low BNF groups. In addition, the expression of *Ahrr* significantly increased in the BNF and OPZ+BNF groups, and significantly increased in the OPZ+BNF group when compared with the OPZ and BNF treated groups.

In phase II metabolic enzymes, the expression of *Akr7a3*, *Gpx2*, *Yc2* and *Me1* significantly increased in the treated groups when compared with the DEN alone group. Of these genes, *Gpx2* and *Yc2* significantly increased in the OPZ+BNF group when compared with the Low OPZ or Low BNF groups. The expression of *Akr7a3* and *Me1* in the OPZ+BNF group showed an increasing tendency when compared with the Low OPZ or Low BNF group (Table 3).

In inflammation-related genes, the expression of *Cox2*, *Serpine1*, *Mmp12* and *Fgf21* significantly increased in the BNF treated groups when compared with the DEN alone groups, and significantly increased or showed an increasing tendency in the OPZ+BNF group when compared with the other treated groups. The expression of *Il-6* showed an increasing tendency in the OPZ+BNF group when compared with the DEN alone group. The expression of *Nfkb1* and *Nfkbia* did not fluctuate in the treated groups but the expression of *Tnf* significantly increased in the High BNF group (Table 3).

In cell cycle-related genes, the expression of *Chek1*

Table 3. Real-time RT-PCR analysis of the liver tissues from male F344 rats given OPZ and/or BNF for 6 weeks after DEN treatment

Group	DEN alone	Low OPZ	High OPZ	Low BNF	High BNF	OPZ+BNF
AhR-regulated genes						
Cyp1a1	1.19 ± 0.67	158.19 ± 197.79$^{**,\#\#}$	138.19 ± 120.20$^{**,\#\#}$	2842.87 ± 824.82**	3357.84 ± 831.00**	3138.85 ± 579.83**
Cyp1a2	1.01 ± 0.18	6.50 ± 1.95$^{**,\#\#}$	6.93 ± 2.83$^{**,\#\#}$	27.79 ± 4.53$^{**,\#\#}$	42.91 ± 6.37**	52.03 ± 11.37**
Cyp1b1	1.06 ± 0.38	4.04 ± 2.15$^{**,\#\#}$	3.28 ± 1.15$^{*,\#\#}$	188.10 ± 50.95$^{**,\#\#}$	706.52 ± 297.60**	1117.09 ± 263.51**
Cyp2b2	1.05 ± 0.34	5.17 ± 1.26$^{**,\#\#}$	6.66 ± 2.57$^{**,\#\#}$	0.66 ± 0.13	0.53 ± 0.17*	0.92 ± 0.40
Aldh1a1	1.08 ± 0.52	3.50 ± 0.92**	3.67 ± 1.45*	1.25 ± 0.12$^{\#\#}$	1.98 ± 0.39*	2.30 ± 0.64*
Aldh3a1	1.23 ± 0.80	1.80 ± 1.02$^{\#\#}$	1.32 ± 0.54$^{\#\#}$	2.56 ± 0.89$^{\#\#}$	90.70 ± 66.77$^{**,\#\#}$	860.74 ± 361.47**
Nqo1	1.03 ± 0.29	2.54 ± 0.88$^{**,\#\#}$	2.81 ± 0.75$^{**,\#\#}$	5.40 ± 0.58$^{**,\#\#}$	10.10 ± 2.85$^{**,\#}$	16.86 ± 3.37**
Ugt1a6	1.03 ± 0.25	1.86 ± 0.35$^{**,\#}$	1.71 ± 0.50$^{*,\#\#}$	1.62 ± 0.18$^{*,\#\#}$	2.45 ± 0.54$^{**,\#}$	3.85 ± 0.86**
Ahrr	2.62 ± 4.31	7.52 ± 3.70$^{\#\#}$	8.62 ± 4.86$^{\#\#}$	55.52 ± 20.05$^{*,\#}$	138.07 ± 52.11*	196.60 ± 71.27*
Nrf2-regulated genes						
Akr7a3	1.01 ± 0.17	3.28 ± 1.03**	4.78 ± 2.18**	1.88 ± 0.71$^{**,\#\#}$	3.25 ± 1.20**	5.75 ± 3.77**
Gpx2	1.04 ± 0.29	4.63 ± 1.5$^{**,\#}$	6.18 ± 1.51**	2.90 ± 0.80$^{**,\#}$	6.89 ± 2.74**	9.18 ± 3.10**
Yc2	1.00 ± 0.10	1.73 ± 0.36$^{**,\#}$	1.73 ± 0.27**	1.26 ± 0.18$^{*,\#\#}$	1.60 ± 0.25$^{**,\#}$	2.42 ± 0.60**
Me1	1.08 ± 0.39	2.35 ± 0.77**	2.57 ± 0.62**	1.94 ± 0.51$^{*,\#}$	1.93 ± 0.88$^{*,\#}$	4.14 ± 2.20**
Inflammation						
Cox2	1.07 ± 0.36	1.52 ± 0.35	1.30 ± 0.22	2.89 ± 0.99**	3.31 ± 1.31**	3.61 ± 1.87*
Serpine1	1.02 ± 0.24	0.95 ± 0.24$^{\#}$	0.99 ± 0.46$^{\#}$	1.59 ± 0.37$^{*,\#}$	2.23 ± 1.18$^{*,\#}$	3.16 ± 0.42**
Mmp12	1.01 ± 0.14	1.01 ± 0.53$^{\#}$	0.90 ± 0.27$^{\#}$	1.26 ± 0.18	2.14 ± 0.65*	2.28 ± 1.24**
Il-6	1.19 ± 0.88	2.12 ± 0.64	1.28 ± 0.80	1.37 ± 0.62	1.37 ± 0.41	2.72 ± 1.98
Fgf21	1.08 ± 0.54	0.94 ± 0.46$^{\#}$	0.94 ± 0.45$^{\#}$	1.68 ± 0.52	1.97 ± 0.80	3.35 ± 2.29*
Nfkb1	1.01 ± 0.16	1.04 ± 0.14	0.94 ± 0.17	0.96 ± 0.07	1.12 ± 0.16	1.00 ± 0.16
Nfkbia	1.1 ± 0.47	1.05 ± 0.39	0.9 ± 0.32	0.6 ± 0.27	0.65 ± 0.17	0.98 ± 0.56
Tnf	1.02 ± 0.22	1 ± 0.2	0.91 ± 0.15	1.23 ± 0.32	1.59 ± 0.26*	1.28 ± 0.46
Cell cycle related genes						
Chek1	1.01 ± 0.17	1.29 ± 0.31	1.41 ± 0.28**	1.14 ± 0.17$^{\#\#}$	1.27 ± 0.34$^{\#}$	1.69 ± 0.34**
Wee1	1.01 ± 0.15	1.36 ± 0.33	1.43 ± 0.34	1.43 ± 0.19	1.60 ± 0.57*	1.86 ± 0.28**
MAP kinase pathway family related genes						
Myc	1.03 ± 0.26	2.59 ± 1.15*	3.00 ± 1.18*	1.10 ± 0.43$^{\#\#}$	1.50 ± 0.52$^{\#}$	3.15 ± 1.62**

DEN, *N*-diethylnitrosamine; Low OPZ, 138 mg/kg omeprazole; High OPZ, 276 mg/kg omeprazole; Low BNF, 0.125% β-naphthoflavone; High BNF, 0.25% β-naphthoflavone; and OPZ+BNF, 138 mg/kg omeprazole + 0.125% β-naphthoflavone. The data represent mean ± S.D.

*, ** significantly different from the DEN alone group at $P < 0.05$ or 0.01.

#, ## significantly different from the OPZ +BNF group at $P < 0.05$ or 0.01.

significantly increased in the High OPZ and OPZ+BNF groups when compared with the DEN alone group, and the expression of *Wee1* significantly increased in the High BNF and OPZ+BNF groups (Table 3).

In other genes, the expression of *Myc* significantly increased in the OPZ and OPZ+BNF groups when compared with the DEN alone group (Table 3).

Microsomal ROS production

To estimate the cellular sources of ROS, NADPH-dependent ROS production was measured in liver microsomes. The oxidized indicator was not detected in the absence of NADPH. With the addition of NADPH into the microsomal system, ROS production was dramatically enhanced, but ROS production significantly decreased in the OPZ treated, high BNF and OPZ+BNF groups when compared with the DEN alone group (Table 2). SKF-525A, a well-known inhibitor of CYP, inhibited NADPH-dependent ROS production.

Oxidative stress on cellular membrane

To evaluate whether oxidative damages to cellular components occurred, TBARS formation was determined in the liver. There was no remarkable change in TBARS content between the groups (Table 2).

Immunohistochemistry of COX-2 in the liver

COX-2-positive cells, which are recognized as Kupffer cells, were observed in the sinusoid of the livers (Fig. 3). COX-2-positive cells were mainly observed in the periportal areas of the liver in the DEN alone group, but were scattered throughout the liver in the BNF and OPZ+BNF groups. In addition, COX-2-positive Kupffer cells were observed in the periphery of some foci of the OPZ+BNF group (Fig 4). The number of COX-2-positive cells in the OPZ+BNF group significantly increased when compared with the DEN alone group (Fig. 3).

Plasma concentration of OPZ and BNF

We estimated the plasma concentration of OPZ and BNF at necropsy (Table 4). In the High BNF and OPZ+BNF groups, the plasma concentration of BNF could not be detected (less than the limit of quantitation: 20 ng/ml). However, the concentration of OPZ was 6,053 ± 2,409 ng/ml in the High OPZ group and 310 ± 241 ng/ml in the OPZ+BNF group.

Experiment 2
Body and liver weights

In all groups, no significant changes in body weights were observed in the treated groups when compared with the MeIQx alone group (Table 5). Absolute liver weights significantly increased in the High BNF group, and relative liver weights significantly increased in the High BNF and OPZ+BNF groups when compared with the DEN alone group (Table 5). The relative liver weights in the OPZ+BNF group significantly increased when compared with the Low OPZ group.

Histopathological examinations and GST-P-positive foci in the liver

Immunohistochemical analysis revealed that the number and area of GST-P-positive foci significantly increased only in the Low BNF group, but not in the High BNF and OPZ+BNF groups (Table 5). Because of there being no dose-relationship in the induction of GST-P-positive foci in BNF treated groups, it was concluded that BNF did not have liver initiation activity. No apparent difference in the localization of GST-P-positive foci with respect to zones 1-3 was observed among the groups. There was no change in the number of PCNA-positive cells among the groups (Table 5).

DISCUSSION

It has previously been demonstrated that the simultaneous administration of several chemicals induced additive or synergistic effects on the carcinogenicity in rats (Hasegawa *et al.*, 1989). The combined administration of hepatocarcinogens such as 2-AAF, benzo[a]pyrene (B[a]

Table 4. Plasma concentration of male F344 rats given OPZ and/or BNF for 6 weeks after DEN treatment

group	plasma OPZ concentration	plasma BNF concentration
High OPZ	3470	BLQ
	6450	BLQ
	8240	BLQ
High BNF	BLQ	BLQ
	BLQ	BLQ
	BLQ	BLQ
OPZ+BNF	203	BLQ
	586	BLQ
	141	BLQ

High OPZ, 276 mg/kg omeprazole; High BNF, 0.25% β-naphthoflavone; and OPZ+BNF, 138 mg/kg omeprazole + 0.125% β-naphthoflavone.
BLQ: Below limit of quantification (less than 20 ng/ml)

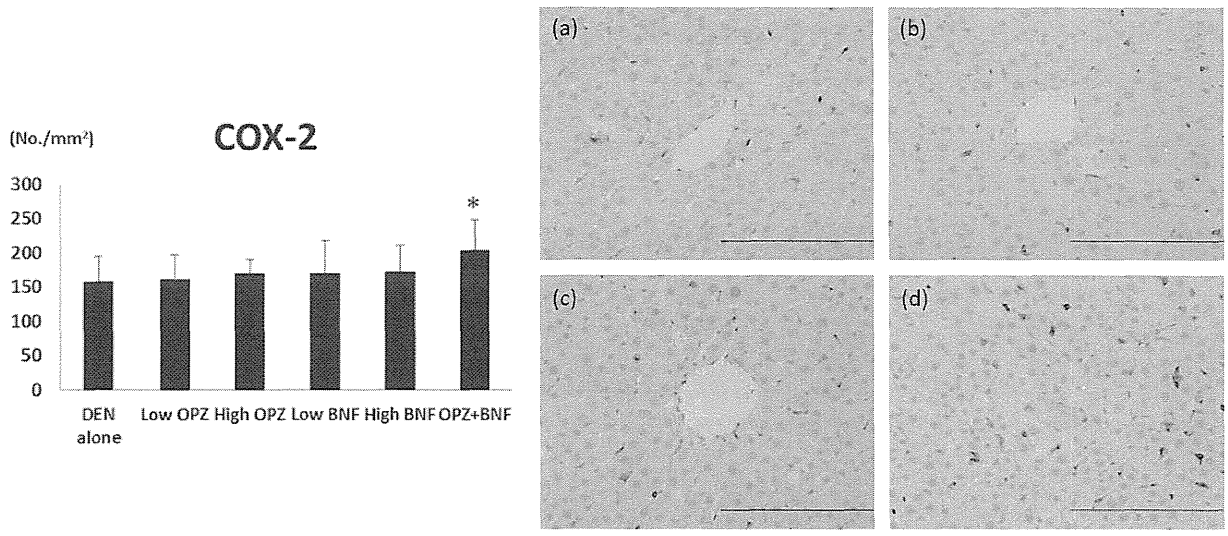

Fig. 3. Immunohistochemical photographs of COX-2 and the number of COX-2-positive cells in the liver of rats given OPZ and/or BNF after DEN initiation. Each photograph shows COX-2-positive cells in the liver of the DEN alone group (a), Low OPZ group (b), Low BNF group (c), and OPZ+ BNF group (d). Original magnification: × 100 (bar: 100 μm). The bar shows mean + S.D. of the number of COX-2 positive-cells in each group. *significantly different from the DEN alone group at $P < 0.05$.

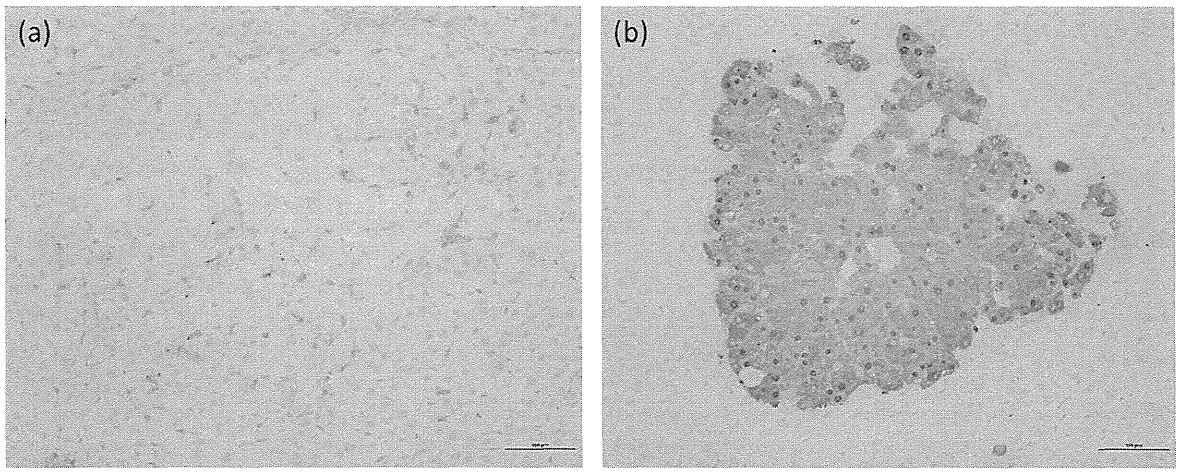

Fig. 4. Immunohistochemical photographs of COX-2 (a) and GST-P (b) in the liver of a rat given OPZ and BNF after DEN initiation. COX-2-positive cells are prominent around the altered focus (a), and the focus gives close agreement with GST-P (b). Original magnification: × 100 (bar: 100 μm).

P) and N-ethyl-N-hydroxyethylnitrosamine at low doses resulted in synergistic effects in the rat liver (Hasegawa *et al.*, 1989). In addition, in the two-stage forestomach carcinogenesis model, the combined administration of promoters/carcinogens exerted a strong enhancing influence on the forestomach carcinogenesis in rats, although the low doses of them did not have a significant promoting activity (Hirose *et al.*, 1991). Synergism occurs when the effect of two or more substances acting together exceeds the sum of their effects when acting separately (Reif *et al.*, 1984). Hasegawa *et al.* (1991) examined potential synergism between five HCAs (3-amino-1-methyl-

Table 5. Final body and liver weights, number/area of GST-P-positive foci, distribution of GST-P-positive foci and number of PCNA-positive cells in the liver of male F344 rats given OPZ and/or BNF for 9 days before MeIQx treatment

Group	MeIQx alone	Low OPZ	High OPZ	Low BNF	High BNF	OPZ+BNF
No. of animals	12	10	12	11	11	11
Final body weight (g)	257.8 ± 9.8	259.2 ± 9.0	254.9 ± 10.6	261.6 ± 13.5	259.8 ± 6.1	256.6 ± 12.9
Absolute liver weight (g)	9.14 ± 0.53	9.37 ± 0.52	9.26 ± 0.62	9.73 ± 0.84	9.87 ± 0.27**	9.59 ± 0.69
Relative liver weight (g/100g body weight)	3.58 ± 0.13	3.59 ± 0.10#	3.61 ± 0.12	3.68 ± 0.19	3.79 ± 0.13**	3.73 ± 0.11*
GST-P-positive foci (≧ 0.2 mm)						
Number (number/cm²)	0.38 ± 0.60	0.18 ± 0.25	0.83 ± 1.24	1.41 ± 1.29*	1.44 ± 1.47	0.78 ± 1.21
Area (mm²/cm²)	0.02 ± 0.03	0.01 ± 0.02	0.06 ± 0.09	0.10 ± 0.09*	0.14 ± 0.22	0.05 ± 0.11
% of GST-P-positive foci for each zone						
Zone 1	0	20.8 ± 25.0	12.5 ± 35.4	13.0 ± 14.5	17.8 ± 21.1	33.4 ± 43.8
Zone 2	68.0 ± 29.5	37.5 ± 47.9	76.0 ± 37.1	51.6 ± 19.3	57.5 ± 29.0	56.7 ± 42.1
Zone 3	32.0 ± 29.5	41.7 ± 44.1	11.5 ± 21.3	39.1 ± 20.6	24.7 ± 20.7	9.9 ± 17.7
PCNA-positive hepatocyte (%)	0.51 ± 0.54	0.40 ± 0.25	0.40 ± 0.48	0.39 ± 0.28	0.50 ± 0.97	0.43 ± 0.36

MeIQx: 2-amino-3,8-dimethylimidazo[4,5-*f*]quinoxaline, Low OPZ: 138 mg/kg omeprazole, High OPZ: 276 mg/kg omeprazole, Low BNF: 0.03% β-naphthoflavone, High BNF: 0.06% β-naphthoflavone, OPZ+BNF: 138 mg/kg omeprazole+0.03% β-naphthoflavone.
The data represent mean ± S.D.
*, ** significantly different from the MeIQx alone group at $P < 0.05$, 0.01.

5*H*-pyrido[4,3-*b*]indole, 2-amino-6-methyldipyrido[1,2-*a*:3',2'-*d*]-imidazole, 2-amino-3-methyl-9*H*-pyrido[2,3-*b*] indole, 2-amino-9*H*-pyrido[2,3-*b*]indole and 2-amino-1-methyl-6-phenylimidazo[4,5-*b*]pyridine). In their report, a heteroadditive model was used, and net values were obtained by subtracting the control value (DEN-alone group). In the heteroadditive model, they compared the net value for the combined treatment and the sum of the net value of individual treatment at 1/5 dose, and the net value for the combined treatment was greater than the sum of net values in 1/5 dose. They concluded that the combination effects were synergistic. However, dose-response curves were not considered in this model. Reif (1984) pointed out the importance of the dose response curve in the analysis of the combined effects, and described that in ordinary heteroadditive methods the combined effect could be evaluated whether it was synergistic or not. In this heteroadditive model, the consideration of the dose response curves was lacking. On the other hand, Hasegawa *et al.* (1994, 1995) examined the combination effect of ten HCAs at low doses using two statistical models, a heteroadditive model and an isoadditive model. In the heteroadditive model, significant greater effects were found in the combination group. On the other hand, in the isoadditive model, Hasegawa *et al.* (1994, 1995) compared the average value of individual treatments of 1/1 dose and the value of ten heterocyclic amines and the combination treatment at 1/10 dose. As a result, since a significant increase was not shown in the combination group, they concluded that this combination effect was not synergistic in the isoadditive model. Futakuchi *et al.* (1996) examined potential synergism between four N-nitroso compounds (nitrosomorpholine, nitrosodimethylamine, nitrosodiethanolamine, and nitroso-oxazolidine) in rat liver carcinogenesis in a medium-term bioassay where male F344 rats were initially given DEN, and 2 weeks later received test chemicals for a period of 6 weeks at a full or 1/4 dose of that proven to be carcinogenic, individually or in combination. In their report, the effect value of individual chemicals was obtained by subtracting the control value (DEN-alone group). In the heteroadditive model, they compared the sum of the effect values of each individual treatment at 1/4 dose and the value for rats treated with four chemicals in combination at the 1/4 dose level, and no significant increase was observed between them. However, in the isoadditive model, the value in combination at the 1/4 dose level treatment was almost the same as the average of four individual treatments at full dose and, the value in combination at 1/16 dose level treatment were not significantly higher than the average value of four individual treatment at 1/4 dose. They concluded that the combined effects were not synergistic but isoadditive. In the present study (Experiment 1), we demonstrated that the combined administration of low doses of OPZ and BNF induced higher numbers of GST-P-positive foci when compared with the high doses of OPZ or BNF, and induced higher areas of GST-P-positive foci when compared with high dose of OPZ. In the heteroadditive model, the effect value of the combination at a low dose (area, 0.67 mm^2/cm^2; number, 8.08 number/cm^2; average of value of OPZ+BNF minus value of DEN-alone) was not significantly higher than the sum of the effect value of both OPZ and BNF at low dose (area, 0.55 mm^2/cm^2; number, 5.34 number/cm^2). However, in the isoadditive model, the value of the combined administration of low doses of OPZ and BNF (area, 0.82 ± 0.34 mm^2/cm^2; number, 10.66 ± 2.76 number/cm^2) was significantly higher ($P < 0.05$, *t* test) than the average value of each individual treatment at a high dose of OPZ and BNF (area, 0.50 ± 0.27 mm^2/cm^2; number, 6.53 ± 2.40 number/cm^2; average of value of High OPZ and value of High BNF). Therefore, it can be concluded that the combined liver tumor promotion effect of OPZ and BNF is synergistic in the isoadditive model.

In Experiment 1, phase I metabolic enzymes such as *Cyp1a1*, *Cyp1a2*, *Cyp1b1*, *Nqo1* and *Ugt1a6*, which are called as AhR gene battery and induced by AhR, significantly increased or showed an increasing tendency in the OPZ+BNF group when compared with the Low OPZ or Low BNF group. Aryl-hydrocarbon receptor repressor (AHRR) is activated by the AhR ligand in heterodimer with aryl hydrocarbon receptor nuclear translocator (ARNT), and expressed AHRR inhibits the AhR function (Brauze *et al.*, 2006). AhR and AHRR constitute a negative regulatory feedback loop of xenobiotic signal transductions (Brauze *et al.*, 2006). In the OPZ+BNF group, the expression of *Ahrr* significantly increased or showed an increasing tendency when compared with the treated groups, suggesting the enhanced transduction of AhR. In addition, phase II metabolic enzymes such as *Akr7a3*, *Gpx2*, *Yc2* and *Me1* significantly increased in the treated groups, and significantly increased or showed an increasing tendency in the OPZ+BNF group when compared with the other treated groups. Nrf2 is activated by oxidative stress and induces detoxification enzymes and antioxidants (Köhle and Bock, 2007). It is generally accepted that the microsomal electron system, including CYPs and NADPH-CYP reductase generates ROS through the metabolism, with the subsequent formation of an oxygenated substrate and water (Poulos and Raag, 1992). Although electron transfer is normally a well-coupled process, superoxide and H_2O_2 may be released in

the presence of CYP1A inducers that are poorly metabolized (Puntarulo and Cederbaum, 1998; Nishikawa *et al.*, 2002). Therefore, upregulation of these genes suggests that the increment of ROS production contributes to the enhancement of the liver tumor promoting effect in the OPZ+BNF group. However, microsomal ROS production significantly decreased in the OPZ+BNF group, and no fluctuations of TBARS were observed in the treated groups. Oxidative stress usually occurs when ROS production in cells or tissues exceeds the antioxidant potential (Klaunig *et al.*, 1998). Therefore, it is possible that the antioxidant regulated by Nrf2 probably exceeds the ROS production and removes the ROS generated in the OPZ+BNF group.

It has been demonstrated in our previous studies that COX-2 is related to the liver tumor promoting effect of BNF (Shimada *et al.*, 2010; Kuwata *et al.*, 2011). COX-2 may be involved in the early stage of hepatocarcinogenesis, and the increased expression of COX-2 in noncancerous liver tissues has been significantly associated with shorter disease-free survival in patients with hepatocellular carcinomas (Cervello and Montalto, 2006). In tumors in human, overexpression of COX-2 leads to an increase in prostaglandin (PG) levels which affects many mechanisms involved in carcinogenesis, such as angiogenesis, inhibition of apoptosis, and stimulation of cell growth, as well as invasiveness and the metastatic potential of tumor cells (Cervello and Montalto, 2006). Several reports suggest that OPZ might have an anti-inflammation effect (Kedika *et al.*, 2009; Shivanna *et al.*, 2011). Indeed, OPZ inhibited ROS production and protected against oxidative stress by inducing *heme-oxygenase-1* (Kedika *et al.*, 2009; Shivanna *et al.*, 2011). However, the ligands of AhR, including TCDD and B[a]P, induced *Cox-2* expression (Degner *et al.*, 2007 and 2009). TCDD and B[a]P induced transcription activity of COX-2 in breast cancer MCF-7 cells (Degner *et al.*, 2007). Furthermore, the TCDD-association of AhR to xenobiotics responsive elements in the *Cox-2/Cyp1a* promoter was inhibited by AhR antagonists such as 3,3'-diindolulmetahane and resveratrol (Denger *et al.*, 2007). On the other hand, TCDD increases the intracellular concentration of free Ca^{2+} and subsequently activates cytosolic phospholipase A2 and additional inflammatory marker, *Cox-2*, expression in U937 macrophages (Sciullo *et al.*, 2008). In the present study, the expression of *Nfkb1*, *Nfkbia* and *Tnf*, which are regulated by Nfkb, did not fluctuate in the OPZ+BNF group. However, the expression of *Cox-2* significantly increased in the OPZ+BNF group when compared with the DEN alone group, and COX-2 protein also significantly increased in this group. Therefore, these data indicate that the activation of AhR contributes to the enhancement of COX-2, and it can be suggested that the combined administration of OPZ and BNF, which are the ligands of AhR, may induce COX-2 via AhR and enhance the liver tumor promoting effect in rats. On the contrary, the induction of *Cyp1a* by AhR was induced in hepatocytes, but it is not clear whether the induction of *Cox-2* in Kupffer cells occurred in the same mechanism. Recently, it has been reported that tumor microenvironment is related to the hepatocarcinogenesis (Yang *et al.*, 2011). Kupffer cells induce programmed death ligand-1, which impairs cytotoxic $CD8^+$ T cell function in human hepatocellular carcinomas (Yang *et al.*, 2011). Kupffer cells also produce IL-6 and osteopontin that play a pivotal role in various cell signaling pathways promoting inflammation, tumor progression and metastasis. Therefore, Kupffer cells expressing COX-2 might have been related to the liver tumor promoting effect.

CHEK1 is phosphorylated in response to DNA damage and is essential for cell-cycle arrest in response to DNA damage or DNA replication blockage (Niida and Nakanishi, 2006). WEE1 is a tyrosine kinase that controls the cell cycle in response to DNA damage (Raleigh and O'Connell, 2000). When DNA damage is induced in the G2 phase, Wee1 phosphorylates cyclin-dependent kinase 2 (cdc2) and inactivates cdc2, and prevents the entry into mitosis phase (Raleigh and O'Connell, 2000). OPZ showed a weak genotoxicity in primary rat hepatocytes (Martelli *et al.*, 1998). In the present study, the expression of *Chek1* and *Wee1* significantly increased in the OPZ+BNF group when compared with the DEN alone group. In addition, the expression of *Myc* significantly increased in the OPZ treated and OPZ+BNF groups. Myc has a neoplastic potential and plays an important role in regulating cell proliferation (Dang, 1999). Impaired expression of Myc is related to the development of many malignant tumors in humans and animals (Hoffman and Liebermann, 1998). OPZ has a liver tumor promoting effect in rats, but the mechanism is not clear. Taking into account these points, it can be considered that the involvement of DNA damage and increased expression of *Myc* are related to the enhancement of liver tumor promoting effects of OPZ and BNF, although further study is needed.

The plasma concentration of BNF could not be detected. However, the concentration of OPZ was 6,053 ± 2,409 ng/ml in the High OPZ group and 310 ± 241 ng/ml in the OPZ+BNF group. OPZ is metabolized via hepatic CYP1A1/2, 2D1, 3A1/2 in rats (Lee *et al.*, 2009). In the OPZ+BNF group, the expression of *Cyp1a1* and *1a2* increased when compared with the Low OPZ and Low

BNF groups. This finding suggests that the induction of liver drug-metabolizing enzyme by BNF may affect the metabolism of OPZ in the OPZ+BNF group. It has previously been shown that the plasma concentration of BNF reaches a maximal level at 80-120 min and then starts declining toward a lower plateau value in SD rats given a continuous intravenous infusion of 1.5 or 6 mg/kg/hr BNF for 6 hr (Chen *et al.*, 2010). BNF is known as a substrate of CYP1A enzymes and the BNF clearance increases with time after continuous intravenous infusion to rats (Chen *et al.*, 2010). Such a time-dependent increase in clearance supports the present finding of plasma BNF concentrations not being detected in BNF treated rats. In addition, the exponential increase of plasma concentration of OPZ was not observed with the combined administration of OPZ and BNF. On the other hand, the expression of *Cyp1a1* in the 0.5% BNF group was 299-fold higher than that of the DEN alone group when they were fasted for 12 hours (Shimamoto *et al.*, 2011b), while the expression of *Cyp1a1* without fasting in the 0.25% BNF group of our study was 3357-fold higher than that of the DEN alone group. Therefore, since the expression of genes such as *Cyp1a1* and *Cyp1a2* significantly increased in the OPZ+BNF group, it is likely that some unknown metabolic effect due to the combined administration intensifies the liver tumor promoting effect.

MeIQx is activated by CYP1A2, and the metabolites produced are highly reactive and bind covalently to DNA (Yamazoe *et al.*, 1988). Previous reports have shown that CYP1A2 inducers such as fenbendazole and caffeine did not enhance the MeIQx-induced hepatocarcinogenesis in rats (Suzuki *et al.*, 2002; Kuribayashi *et al.*, 2006). It has also been reported that BNF did not enhance the MeIQx-induced hepatocarcinogenesis in rats (Suzuki *et al.*, 2010). In that study, CYP1A expression was mainly observed in the area adjacent to the central veins (zone 3) of the liver, where GST-P-positive foci were preferentially located, in MeIQx-treated rats; while BNF treatment induced CYP1A in the area adjacent to Glisson's sheath (zone 1). Taken into account the distribution differences of the CYP1A induction between MeIQx and BNF, Suzuki *et al.* (2010) speculated that the difference of CYP1A expression may be related to MeIQx-induced hepatocarcinogenesis. In the present study, no apparent difference in distribution of GST-P-positive foci was observed among the groups. Although CYP1A2 activates MeIQx, CYP1A1 is thought to be related to the detoxification of MeIQx (Suzuki *et al.*, 2002). Indole-3-carbinol, which is a chemopreventive compound, preferentially induces CYP1A1 rather than CYP1A2 and inhibits the HCA-induced carcinogenicity by shifting the metabolism of HCAs (Hirata *et al.*, 2008). In our previous studies, OPZ and BNF also induced expression of both *Cyp1a1* and *Cyp1a2* in rats, and preferentially induced *Cyp1a1* rather than *Cyp1a2* (Hayashi *et al.*, 2012a, 2012b). In addition, the expression of NATs in the liver did not fluctuate with the administration of BNF (Suzuki *et al.*, 2002). Because MeIQx is activated by NAT, no induction of NAT may result in the unchanged initiation activities. In the present study, no enhancement of MeIQx-induced hepatocarcinogenesis was observed in the OPZ+BNF group, although the number and area of GST-P-positive foci increased in the Low BNF group but not in the High BNF group. Therefore, enhanced liver initiation activity may not be induced by the treatment of two different chemicals that have similar capabilities to induce both CYP1A1 and CYP1A2.

In conclusion, the co-administration of OPZ and BNF resulted in an enhanced liver tumor promoting effect but not liver initiation activity in rats. The outcome of the present study suggests the possibility that the combined liver tumor promotion effect of two different compounds that have similar capabilities to induce CYP1A is synergistic. Currently, regulatory agencies in individual countries set the acceptable daily intake for chemicals in food. However, particular attention should be paid to the combined exposure of plural chemicals in food that are recognized as CYP inducers. In order to eliminate the enhanced adverse effects from simultaneous exposure to plural chemicals that have the capability of inducing CYPs, we must reconsider the risk evaluation of these chemicals. As our data are limited to the combined administration of OPZ and BNF only, further examination using other CYP inducers is vital.

ACKNOWLEDGMENT

This study was partly supported by a grant in-aid for research on the safety of veterinary drugs in food of animal origin from the Ministry of Health, Labour and Welfare of Japan (H22-Shokuhin-Ippan-007).

Supplementary data

Supplementary data associated with this article can be found in the online version.

REFERENCES

Brauze, D., Widerak, M., Cwykiel, J., Szyfter, K. and Baer-Dubowska, W. (2006): The effect of aryl hydrocarbon receptor ligands on the expression of AhR, AhRR, ARNT, Hif1alpha, CYP1A1 and NQO1 genes in rat liver. Toxicol. Lett., **167**, 212-220.

Cervello, M. and Montalto, G. (2006): Cyclooxygenases in hepatocellular carcinoma. World J. Gastroenterol., **12**, 5113-5121.

Chen, E.P., Chen, L., Ji, Y., Tai, G., Wen, Y.H. and Ellens, H. (2010): A mechanism-based mathematical model of aryl hydrocarbon receptor-mediated CYP1A induction in rats using beta-naphthoflavone as a tool compound. Drug Metab. Dispos., **38**, 2278-2285.

Dang, C.V. (1999): c-Myc target genes involved in cell growth, apoptosis, and metabolism. Mol. Cell. Biol., **19**, 1-11.

Degner, S.C., Kemp, M.Q., Hockings, J.K. and Romagnolo, D.F. (2007): Cyclooxygenase-2 promoter activation by the aromatic hydrocarbon receptor in breast cancer mcf-7 cells: repressive effects of conjugated linoleic acid. Nutr. Cancer., **59**, 248-257.

Degner, S.C., Papoutsis, A.J., Selmin, O. and Romagnolo, D.F. (2009): Targeting of aryl hydrocarbon receptor-mediated activation of cyclooxygenase-2 expression by the indole-3-carbinol metabolite 3,3'-diindolylmethane in breast cancer cells. J. Nutr., **139**, 26-32.

Dewa, Y., Nishimura, J., Muguruma, M., Jin, M., Saegusa, Y., Okamura, T., Tasaki, M., Umemura, T. and Mitsumori, K. (2008): Beta-Naphthoflavone enhances oxidative stress responses and the induction of preneoplastic lesions in a diethylnitrosamine-initiated hepatocarcinogenesis model in partially hepatectomized rats. Toxicology, **244**, 179-189.

Dewa, Y., Nishimura, J., Muguruma, M., Jin, M., Kawai, M., Saegusa, Y., Okamura, T., Umemura, T. and Mitsumori, K. (2009): Involvement of oxidative stress in hepatocellular tumor-promoting activity of oxfendazole in rats. Arch. Toxicol., **83**, 503-511.

Futakuchi, M., Lijinsky, W., Hasegawa, R., Hirose, M., Ito, N. and Shirai, T. (1996): Effects of low dose mixtures of four N-nitroso compounds on hepatic foci development in the rat. Cancer Lett., **106**, 263-269.

Hayashi, H., Shimamoto, K., Taniai, E., Ishii, Y., Morita, R., Suzuki, K., Shibutani, M. and Mitsumori, K. (2012a): Liver tumor promoting effect of omeprazole in rats and its possible mechanism of action. J. Toxicol. Sci., **37**, 491-501.

Hayashi, H., Taniai, E., Morita, R., Yafune, A., Suzuki, K., Shibutani, M. and Mitsumori, K. (2012b): Threshold dose of liver tumor promoting effect of β-naphthoflavone in rats. J. Toxicol. Sci., **37**, 517-526.

Hasegawa, R., Miyata, E., Futakuchi, M., Hagiwara, A., Nagao, M., Sugimura, T. and Ito, N. (1994): Synergistic enhancement of hepatic foci development by combined treatment of rats with 10 heterocyclic amines at low doses. Carcinogenesis, **15**, 1037-1041.

Hasegawa, R., Mutai, M., Imaida, K., Tsuda, H., Yamaguchi, S. and Ito, N. (1989) Synergistic effects of low-dose hepatocarcinogens in induction of glutathione S-transferase P-positive foci in the rat liver. Jpn. J. Cancer Res., **80**, 945-951.

Hasegawa, R., Shirai, T. and Ito, N. (1995): Enhancement of liver carcinogenesis by combined treatment of rats with heterocyclic amines. Environ. Mutat. Res. Commun., **17**, 83-91.

Hasegawa, R., Shirai, T., Hakoi, K., Takaba, K., Iwasaki, S., Hoshiya, T., Ito, N., Nagao, M. and Sugimura, T. (1991): Synergistic enhancement of glutathione S-transferase placental form-positive hepatic foci development in diethylnitrosamine-treated rats by combined administration of five heterocyclic amines at low doses. Jpn. J. Cancer Res., **82**, 1378-1384.

Hirata, A., Tsukamoto, T., Sakai, H., Takasu, S., Ban, H., Imai, T., Totsuka, Y., Nishigaki, R., Wakabayashi, K., Yanai, T., Masegi, T. and Tatematsu, M. (2008): Carcinogenic risk of heterocyclic amines in combination - assessment with a liver initiation model. Food Chem. Toxicol., **46**, 2003-2009.

Hirose, M., Mutai, M., Takahashi, S., Yamada, M., Fukushima, S. and Ito, N. (1991): Effects of phenolic antioxidants in low dose combination on forestomach carcinogenesis in rats pretreated with N-methyl-N'-nitro-N-nitrosoguanidine. Cancer Res., **51**, 824-827.

Hoffman, B. and Liebermann, D.A. (1998): The proto-oncogene c-myc and apoptosis. Oncogene, **17**, 3351-3357.

Irizarry, R.A., Hobbs, B., Collin, F., Beazer-Barclay, Y.D., Antonellis, K.J., Scherf, U. and Speed, T.P. (2003): Exploration, normalization, and summaries of high density oligonucleotide array probe level data. Biostatistics, **4**, 249-264.

Ito, N., Tamano, S. and Shirai, T. (2003): A medium-term rat liver bioassay for rapid *in vivo* detection of carcinogenic potential of chemicals. Cancer Sci., **94**, 3-8.

Kato, R. and Yamazoe, Y. (1987): Metabolic activation and covalent binding to nucleic acids of carcinogenic heterocyclic amines from cooked foods and amino acid pyrolysates. Jpn. J. Cancer Res., **78**, 297-311.

Kedika, R.R., Souza, R.F. and Spechler, S.J. (2009): Potential anti-inflammatory effects of proton pump inhibitors: a review and discussion of the clinical implications. Dig. Dis. Sci., **54**, 2312-2317.

Klaunig, J.E., Xu, Y., Isenberg, J.S., Bachowski, S., Kolaja, K.L., Jiang, J., Stevenson, D.E. and Walborg, E.F.Jr. (1998): The role of oxidative stress in chemical carcinogenesis. Environ. Health Perspect., **106**, **Suppl. 1**, 289-295.

Kociba, R.J., Keyes, D.G., Beyer, J.E., Carreon, R.M., Wade, C.E., Dittenber, D.A., Kalnins, R.P., Frauson, L.E., Park, C.N., Barnard, S.D., Hummel, R.A. and Humiston, C.G. (1978): Results of a two-year chronic toxicity and oncogenicity study of 2,3,7,8-tetrachlorodibenzo-p-dioxin in rats. Toxicol. Appl. Pharmacol., **46**, 279-303.

Köhle, C. and Bock, K.W. (2007): Coordinate regulation of Phase I and II xenobiotic metabolisms by the Ah receptor and Nrf2. Biochem. Pharmacol., **73**, 1853-1862.

Kuribayashi, M., Asamoto, M., Suzuki, S., Hokaiwado, N., Ogawa, K. and Shirai, T. (2006): Lack of modification of 2-amino-3,8-dimethylimidazo[4,5-f]quinoxaline (MeIQx) rat hepatocarcinogenesis by caffeine, a CYP1A2 inducer, points to complex counteracting influences. Cancer Lett., **232**, 289-299.

Kuwata, K., Shibutani, M., Hayashi, H., Shimamoto, K., Hayashi, S.M., Suzuki, K. and Mitsumori K. (2011): Concomitant apoptosis and regeneration of liver cells as a mechanism of liver-tumor promotion by β-naphthoflavone involving TNFα-signaling due to oxidative cellular stress in rats. Toxicology, **283**, 8-17.

Lee, D.Y., Jung, Y.S., Kim, Y.C., Kim, S.Y. and Lee, M.G. (2009): Faster clearance of omeprazole in mutant Nagase analbuminemic rats: possible roles of increased protein expression of hepatic CYP1A2 and lower plasma protein binding. Biopharm. Drug Dispos., **30**, 107-116.

Livak, K.J. and Schmittgen, T.D. (2001): Analysis of relative gene expression data using real-time quantitative PCR and the 2(-Delta Delta C(T)) Method. Methods., **25**, 402-408.

Lynch, A.M., Knize, M.G., Boobis, A.R., Gooderham, N.J., Davies, D.S. and Murray, S. (1992): Intra- and interindividual variability in systemic exposure in humans to 2-amino-3,8-dimethylimidazo[4,5-f]quinoxaline and 2-amino-1-methyl-6-phenylimidazo[4,5-b]pyridine, carcinogens present in cooked beef. Cancer Res., **52**, 6216-6223.

Ma, Q. and Lu, A.Y. (2007): CYP1A induction and human risk assessment: an evolving tale of *in vitro* and *in vivo* studies. Drug Metab. Dispos., **35**, 1009-1016.

Martelli, A., Mattioli, F., Mereto, E., Brambilla, Campart, G., Sini, D., Bergamaschi, G. and Brambilla, G. (1998): Evaluation of omeprazole genotoxicity in a battery of *in vitro* and *in vivo* assays. Toxicology, **130**, 29-41.

Niida, H. and Nakanishi, M. (2006): DNA damage checkpoints in mammals. Mutagenesis, **21**, 3-9

Nishikawa, T., Wanibuchi, H., Ogawa, M., Kinoshita, A., Morimura, K., Hiroi, T., Funae, Y., Kishida, H., Nakae, D. and Fukushima, S. (2002): Promoting effects of monomethylarsonic acid, dimethylarsinic acid and trimethylarsine oxide on induction of rat liver preneoplastic glutathione S-transferase placental form positive foci: a possible reactive oxygen species mechanism. Int. J. Cancer, **100**, 136-139.

Ohkawa, H., Ohishi, N. and Yagi, K. (1979): Assay for lipid peroxides in animal tissues by thiobarbituric acid reaction. Anal. Biochem., **95**, 351-358.

Poulos, T.L. and Raag, R. (1992): Cytochrome P450cam: crystallography, oxygen activation, and electron transfer. FASEB J., **6**, 674-679.

Puntarulo, S. and Cederbaum, A.I. (1998): Production of reactive oxygen species by microsomes enriched in specific human cytochrome P450 enzymes. Free Radic. Biol. Med., **24**, 1324-1330.

Raleigh, J.M. and O'Connell, M.J. (2000): The G(2) DNA damage checkpoint targets both Wee1 and Cdc25. J. Cell. Sci., **113**, 1727-1736.

Reif, A.E. (1984): Synergism in carcinogenesis. J. Natl. Cancer Inst., **73**, 25-39.

Schlezinger, J.J., White, R.D. and Stegeman, J.J. (1999): Oxidative inactivation of cytochrome P-450 1A (CYP1A) stimulated by 3,3',4,4'-tetrachlorobiphenyl: production of reactive oxygen by vertebrate CYP1As. Mol. Pharmacol., **56**, 588-597.

Sciullo, E.M., Vogel, C.F., Li, W. and Matsumura, F. (2008): Initial and extended inflammatory messages of the nongenomic signaling pathway of the TCDD-activated Ah receptor in U937 macrophages. Arch. Biochem. Biophys., **480**, 143-155.

Shimada, Y., Dewa, Y., Ichimura, R., Suzuki, T., Mizukami, S., Hayashi, S.M., Shibutani, M. and Mitsumori, K. (2010): Antioxidant enzymatically modified isoquercitrin suppresses the development of liver preneoplastic lesions in rats induced by beta-naphthoflavone. Toxicology, **268**, 213-218.

Shimamoto, K., Dewa, Y., Ishii, Y., Kemmochi, S., Taniai, E., Hayashi, H., Imaoka, M., Morita, R., Kuwata, K., Suzuki, K., Shibutani, M. and Mitsumori, K. (2011a): Indole-3-carbinol enhances oxidative stress responses resulting in the induction of preneoplastic liver cell lesions in partially hepatectomized rats initiated with diethylnitrosamine. Toxicology, **283**, 109-117.

Shimamoto, K., Dewa, Y., Kemmochi, S., Taniai, E., Hayashi, H., Imaoka, M., Shibutani, M. and Mitsumori, K. (2011b): Relationship between CYP1A induction by indole-3-carbinol or flutamide and liver tumor-promoting potential in rats. Arch. Toxicol., **85**, 1159-1166.

Shivanna, B., Chu, C., Welty, S.E., Jiang, W., Wang, L., Couroucli, X.I. and Moorthy, B. (2011): Omeprazole attenuates hyperoxic injury in H441 cells via the aryl hydrocarbon receptor. Free Radic. Biol. Med., **51**, 1910-1917.

Suzuki, S., Takahashi, S., Asamoto, M., Inaguma, S., Ogiso, T., Hirose, M. and Shirai, T. (2002): Lack of modification of 2-amino-3,8-dimethylimidazo[4,5-f]quinoxaline (MeIQx)-induced hepatocarcinogenesis in rats by fenbendazole--a CYP1A2 inducer. Cancer Lett., **185**, 39-45.

Suzuki, S., Takeshita, K., Doi, Y., Asamoto, M., Takahashi, S., Naiki-Ito, A. and Shirai, T. (2010): 2-Amino-3,8-dimethylimidazo[4,5-f]quinoxaline (MeIQx)-induced hepatocarcinogenesis is not enhanced by CYP1A inducers, alpha- and beta-naphthoflavone: relationship to intralobular distribution of CYP1A expression. Toxicol. Pathol., **38**, 583-591.

Tsuda, H., Lee, G. and Farber, E. (1980): Induction of resistant hepatocytes as a new principle for a possible short-term *in vivo* test for carcinogens. Cancer Res., **40**, 1157-1164.

Tsuda, H., Sekine, K., Uehara, N., Takasuka, N., Moore, M.A., Konno, Y., Nakashita, K. and Degawa, M. (1999): Heterocyclic amine mixture carcinogenesis and its enhancement by caffeine in F344 rats. Cancer Lett., **143**, 229-234.

Yamazoe, Y., Abu-Zeid, M., Manabe, S., Toyama, S. and Kato, R. (1988): Metabolic activation of a protein pyrolysate promutagen 2-amino-3,8-dimethylimidazo[4,5-f]quinoxaline by rat liver microsomes and purified cytochrome P-450. Carcinogenesis, **9**, 105-109.

Yanagawa, Y., Sawada, M., Deguchi, T., Gonzalez, F.J. and Kamataki, T. (1994): Stable expression of human CYP1A2 and N-acetyltransferases in Chinese hamster CHL cells: mutagenic activation of 2-amino-3-methylimidazo[4,5-f]quinoline and 2-amino-3,8-dimethylimidazo[4,5-f]quinoxaline. Cancer Res., **54**, 3422-3427.

Yang, J.D., Nakamura, I. and Roberts, L.R. (2011): The tumor microenvironment in hepatocellular carcinoma: current status and therapeutic targets. Semin Cancer Biol., **21**, 35-43.

Yoshihara, S., Makishima, M., Suzuki, N. and Ohta, S. (2001): Metabolic activation of bisphenol A by rat liver S9 fraction. Toxicol. Sci., **62**, 221-227.

The Journal of Toxicological Sciences (J. Toxicol. Sci.)
Vol.38, No.3, 403-413, 2013

Original Article

Liver tumor promoting effect of orphenadrine in rats and its possible mechanism of action including CAR activation and oxidative stress

Reiko Morita[1,2], Atsunori Yafune[1,2], Ayako Shiraki[1,2], Megu Itahashi[1,2], Yuji Ishii[3], Hirotoshi Akane[1], Fumiyuki Nakane[1], Kazuhiko Suzuki[4], Makoto Shibutani[1] and Kunitoshi Mitsumori[1]

[1]Laboratory of Veterinary Pathology, Tokyo University of Agriculture and Technology, 3-5-8 Saiwai-cho, Fuchu-shi, Tokyo 183-8509, Japan
[2]Pathogenetic Veterinary Science, United Graduate School of Veterinary Sciences, Gifu University, 1-1 Yanagido, Gifu-shi, Gifu 501-1193, Japan
[3]Division of Pathology, National Institute of Health Sciences, 1-18-1 Kamiyoga, Setagaya-ku, Tokyo, 158-8501, Japan
[4]Laboratory of Veterinary Toxicology, Tokyo University of Agriculture and Technology, 3-5-8 Saiwai-cho, Fuchu-shi, Tokyo 183-8509, Japan

(Received January 23, 2013; Accepted March 6, 2013)

ABSTRACT — Orphenadrine (ORPH), an anticholinergic agent, is a cytochrome P450 (CYP) 2B inducer. CYP2B inducers are known to have liver tumor-promoting effects in rats. In this study, we performed a rat two-stage liver carcinogenesis bioassay to examine the tumor-promoting effect of ORPH and to clarify its possible mechanism of action. Male rats were given a single intraperitoneal injection of *N*-diethylnitrosamine (DEN) as an initiation treatment. Two weeks after DEN administration, rats were fed a diet containing ORPH (0, 750, or 1,500 ppm) for 6 weeks. One week after the ORPH-administration rats were subjected to two-thirds partial hepatectomy for the acceleration of hepatocellular proliferation. The number and area of glutathione *S*-transferase placental form-positive foci significantly increased in the DEN-ORPH groups. Real-time RT-PCR revealed increased mRNA expression levels of *Cyp2b1/2*, *Mrp2* and *Cyclin D1* in the DEN-ORPH groups and of *Gpx2* and *Gstm3* in the DEN-High ORPH group. Microsomal reactive oxygen species (ROS) production and oxidative stress markers such as thiobarbituric acid-reactive substances and 8-hydroxydeoxyguanosine were increased in the DEN-High ORPH group. Immunohistochemically, constitutively active/androstane receptor (CAR) were clearly localized in the nuclei of hepatocytes in the DEN-ORPH groups. These results suggest that ORPH causes nuclear translocation of CAR resulting in the induction of the liver tumor-promoting activity. Furthermore, oxidative stress resulting from ROS production is also involved in the liver tumor-promoting activity of ORPH.

Key words: Orphenadrine, Cytochrome P450 2B inducer, Constitutive active/androstane receptor, Reactive oxygen species, Liver tumor, Rat

INTRODUCTION

Orphenadrine (ORPH), a derivative of the antihistamine diphenhydramine, is an anticholinergic agent that is antagonistic to the central and peripheral muscarinic receptors. It is used in the early stages of Parkinson's disease because of its skeletal muscle relaxant properties, and is also used as an analgesic in a variety of musculoskeletal conditions (Brocks, 1999). Since this agent has been approved as a drug in the 1950s, information on the genotoxicity study results is not available. On the other hand, ORPH induces cytochrome P450 family 2 subfamily B (CYP2B) in the livers of rats, and the induction of CYP2B is dependent on the nuclear translocation of the constitutive active/androstane receptor (CAR) (Murray *et al.*, 2003).

Correspondence: Reiko Morita (E-mail: rmorita@cc.tuat.ac.jp)

Phenobarbital (PB), one of the CYP2B inducers, is a liver tumor promoter related to the nuclear translocation of CAR and to oxidative DNA damage resulting from the generation of microsomal reactive oxygen species (ROS). It has been reported that treatment with PB increased mRNA expression and protein levels of CYP2B in a two-stage liver carcinogenesis bioassay in rats (Kinoshita *et al.*, 2003; Waxman and Azaroff, 1992). The nuclear translocation of CAR induced by PB stimulates the expression of various genes that enhance hepatic tumor promotion (Deguchi *et al.*, 2009; Kawamoto *et al.*, 1999). In addition, it has been shown that microsomal ROS production and production of thiobarbituric acid-reactive substances (TBARS) and 8-hydroxydeoxyguanosine (8-OHdG) are induced by PB with increasing the *Cyp2b* (Morita *et al.*, 2011). Taking these facts into account, we hypothesize that ORPH has a liver tumor-promoting activity similar to the activity of PB.

In this study, we performed a two-stage liver carcinogenesis bioassay in rats to examine the hepatic tumor-promoting effect of ORPH and to clarify the possible mechanism of action, with a particular focus on the gene expression and biochemical events of ROS generation, and TBARS and 8-OHdG production in the liver. Additionally, we analyzed the localization of CAR protein expression in hepatocytes and the expression of CAR related-genes in the liver.

MATERIALS AND METHODS

Chemicals

Orphenadrine citrate salt (ORPH; CAS No.4682-36-4, purity: > 99%) was purchased from Sigma-Aldrich (St. Louis, MO, USA). *N*-diethylnitrosamine (DEN; CAS No. 55-18-5, purity: > 99%) was purchased from Tokyo Kasei Kogyo (Tokyo, Japan).

Animals and experimental design

Animals received humane care according to the Guide for Animal Experimentation of the Tokyo University of Agriculture and Technology. Five-week-old male F344/N rats were purchased from Japan SLC, Inc. (Shizuoka, Japan). Rats were housed in cages on clean racks with up to 4 rats per cage, in an air-conditioned room with a 12-hr light/dark cycle (40-70% humidity, and 20-26°C temperature), and had free access to a basal diet (Oriental MF; Oriental Yeast Industries Co., Ltd., Tokyo, Japan) and tap water. After a one-week acclimatization period, a two-stage liver carcinogenesis model was performed as follows: Forty four animals were divided into four groups consisting of 8 (control group), 12 (DEN-alone group), 12 (DEN-Low ORPH group) and 12 (DEN-High ORPH group) animals. All animals except those in the control group received an intraperitoneal injection of 200 mg DEN/kg body weight dissolved in saline to initiate hepatocarcinogenesis. After 2 weeks on the basal diet and tap water, animals in the ORPH-treated groups were fed a diet containing either 750 or 1,500 ppm ORPH for 6 weeks. All animals were subjected to two-thirds partial hepatectomy for acceleration of hepatocellular proliferation 1 week after ORPH treatment. During the partial hepatectomy, one rat each in the DEN-alone and DEN-Low ORPH groups died because of technical errors. Two weeks after the partial hepatectomy one rat in the control group died. For selection of the ORPH dosage we referred to a previous report (Murray *et al.*, 2003). The highest dosage in our study was set at half of the dosage calculated from the report because of the taste of ORPH. At the end of the experiment, the rats were euthanized by exsanguination under ether anesthesia, and the livers were excised and weighed. Sliced liver samples were fixed in 4% phosphate-buffered paraformaldehyde for histopathology and immunohistochemistry. The remaining pieces of the livers were frozen in liquid nitrogen and stored at -80°C until further analysis.

Histopathology and immunohistochemistry

The fixed liver slices were washed with phosphate buffered saline, dehydrated with graded ethanol, embedded in paraffin, and sectioned for histopathological and immunohistochemical examinations. Hematoxylin and eosin (HE) staining was conducted according to routine histopathological methods. In addition, immunohistochemical staining of glutathione *S*-transferase placental form (GST-P), proliferating cell nuclear antigen (PCNA) and CAR was performed by the following procedure: Deparaffinized liver sections were treated with 0.3% H_2O_2 in methanol at room temperature for 30 min to block endogenous peroxidase, and then incubated overnight at 4°C with rabbit anti-GST-P antibody (1:1,000 dilution; Medical and Biological Laboratories Co., Ltd., Aichi, Japan), mouse anti-PCNA antibody (1:500 dilution; Dako, Glostrup, Denmark) or mouse anti-CAR1/2 antibody (1:50 dilution, Santa Cruz Biotechnology, Inc., Dallas, TX, USA). The sections were heated by microwave at 90°C for 10 min for PCNA staining or autoclaved at 120°C for 100 sec for CAR1/2 staining, in 10 mmol/l citrate buffer (pH 6.0) before quenching the endogenous peroxidase activity. The avidin-biotin-peroxidase complex method (Vectastain Elite ABC system; Vector Laboratories, Burlingame, CA, USA) was then employed with 3,3-diaminobenzidine as a chromogen, followed by light counterstaining with hema-

toxylin. The number and areas of GST-P positive foci (> 0.2 mm diameter) and the total areas of the liver sections were measured using the WinRoof software (Mitani Corp., Fukui, Japan). The number of nuclei that were strongly positive for PCNA was counted for 10 random fields (approximately 700-900 hepatocytes in each field) per animal, and their % values were shown as the PCNA positive ratio.

cDNA microarray analysis

Total RNA was extracted with RNeasy Mini Kits (Qiagen, Hilden, Germany), according to the manufacturer's instructions. Using 10 μg of total RNA from one animal each of the control, DEN-alone and DEN-High ORPH groups, double-stranded cDNA was synthesized with the Superscript Double-Stranded cDNA Synthesis kit (Invitrogen Corp., Carlsbad, CA, USA), according to the manufacturer's protocol. After labeling with Cy3, 6 μg of each Cy3-labeled cDNA sample was loaded onto the *Rattus norvegicus* Roche NimbleGen microarray for Gene Expression (Roche NimbleGen., Madison, WI, USA: Euk Expr 385K catalog Arr, 26,739 targets/microarray). Differentially expressed genes were analyzed using the Robust Multiple Average (RMA) normalization method (Irizarry *et al.*, 2003). Gene information was retrieved from the National Center for Biotechnology Information (http://www.ncbi.nlm.nih.gov) websites.

Real-time reverse transcription polymerase chain reaction (RT-PCR) analysis

Expression of the genes listed in Table 1 was quantified using quantitative real-time reverse transcription polymerase chain reaction (RT-PCR) analysis. Briefly, the total RNA from six rats in each group was extracted using RNeasy Mini Kits (Qiagen) according to the manufacturer's instructions. The total RNA was reversely transcribed by using ThermoScript reverse transcriptase (Super Script III First-Strand Synthesis System; Invitrogen). All PCR reactions were performed using the *Power* SYBR® Green PCR Master Mix (Applied Biosystems Japan Ltd., Tokyo, Japan) and were carried out using an Applied Biosystems StepOnePlus™ Real-Time PCR System (Applied Biosystems Japan Ltd.) under the following conditions: one cycle at 50°C for 2 min followed by 95°C for 10 min, and 40 cycles at 95°C for 15 sec and 60°C for 1 min. The forward and reverse primers listed in Table 1 were designed using the Primer Express 3.0 software following Applied Biosystems' instructions for optimal primer design. The relative differences in gene expression were calculated using the cycle time (Ct) values that were first normalized with those of actin beta, the endogenous control in the same sample, and then relative to a control Ct value by a $2^{-\Delta\Delta C_t}$ method (Livak and Schmittgen, 2001) using the StepOnePlus software (Applied Biosystems Japan Ltd.). The data are presented as the average fold changes with standard deviation.

Table 1. Primers used for real-time RT-PCR

Accession no.	Gene description	Gene symbol	Forward (5' → 3')	Reverse (5' → 3')
NM_012540	Cytochrome P450, family 1, subfamily a, polypeptide 1	*Cyp1a1*	gccttcacatcagccacaga	ttgtgactctaaccacccagaatc
NM_001198676	Cytochrome P450, family 2, subfamily b, polypeptide1and 2	*Cyp2b1/2*	gggacactgaaaaagagtgaagct	aatgccttcgccaagacaaat
NM_183403.2	Glutathione peroxidase 2	*Gpx2*	gtgtgatgtcaatgggcagaat	agggcagcttgtctttcaggta
NM_020540.1	Glutathione *S*-transferase mu 3	*Gstm3*	gaacgttcgcggacttactca	acgtatctcttctcctcatagtttgaatct
NM_022941	Nuclear receptor subfamily 1, group I, member 3	*Nr1i3 (CAR)*	catttccatgccctgacttgtg	aggctggacaatggcgtctc
NM_012833	ATP-binding cassette, subfamily C, member 2	*Abcc2 (Mrp2)*	gtggtccatacttttcatcatcctt	aagcactcagccagaggttagag
NM_171992	Cyclin D1	*Cyclin D1 (Ccnd1)*	cccacgatttcatcgaacact	gtgcatgtttgcggatgatct
NM_131906	Solute carrier organic anion transporter family, member 1a4	*Slco1a4 (Slc21a5)*	ggctctgcctgtctgagtacctt	ttgttaagcctgccactggaa
NM_031144	Actin, beta	*Actb*	ccctggctcctagcaccat	agagccaccaatccacacaga

Microsomal reactive oxygen species (ROS) production

Microsomal fractions were obtained according to the method of Yoshihara *et al.* (2001). Briefly, liver samples from six rats in each group were homogenized with three volumes of ice-cold 1.15% KCl-0.05 mol/l Tris-HCl buffer (pH 7.4) using TissueLyser II (Qiagen). The homogenate was centrifuged at 3,000 rpm for 10 min, and the supernatant was centrifuged at 11,000 rpm for 20 min. The resultant supernatant was further centrifuged at 51,000 rpm for 90 min. Finally, the pellet was resuspended in 1.15% KCl-0.05 mol/l Tris-HCl buffer (pH 7.4) as the microsomal fraction and stored at -80°C. Microsomal protein concentrations were determined by a BCA Protein Assay Kits (Pierce, IL, USA).

ROS was measured by the partially modified method of Serron *et al.* (2000). Microsomes (final concentration 0.2 mg/ml) were incubated in the dark at 37°C in 40 mM Tris buffer (pH 7.4) and 5 μM 2',7'-dichlorodihydro-fluorescein diacetate (H_2DCFHDA, Invitrogen). At the end of the incubation period, H_2O_2 (final concentration 0.1 mM) as a positive control or SKF-525A (final concentration 0.1 mM, Toronto Research Chemicals, North York, ON, Canada), a well-known inhibitor of cytochrome P450, were added, and the samples were further incubated at 37°C for 30 min in the dark. After that, nicotinamide adenine dinucleotide phosphate (NADPH; final concentration 0.5 mM; Oriental Yeast Co., Ltd., Tokyo, Japan) was added, and the rate at which ROS formed the fluorescent product was measured using a Synergy HT Multi-Detection Microplate Reader (BioTek, Winooski, VT, USA) with excitation and emission wavelengths of 485 and 528 nm, respectively. The data were normalized to control values expressed as 100%.

Determination of 8-OHdG and TBARS levels

Oxidative DNA damage and lipid peroxidation in the livers were estimated by the levels of 8-OHdG and TBARS, respectively.

The 8-OHdG level in liver DNA was determined in six liver samples from each of the DEN-alone and DEN-High ORPH groups using the method of Umemura *et al.* (2006). Briefly, nuclear DNA was isolated from 0.3 g of the wet weight samples using a DNA Extractor WB Kit (Wako Pure Chemical Industries., Osaka, Japan) containing an antioxidant NaI solution to dissolve the cellular components. For further prevention of autoxidation in the cell-lysis step, deferoxamine mesylate was added to the lysis buffer (Helbock *et al.*, 1998). The DNA was digested into deoxynucleotides with nuclease P1 and alkaline phosphatase. The levels of 8-OHdG (8-OHdG/10^5 deoxyguanosine) were then assessed by high-performance liquid chromatography with an electrochemical detection system (Coulochem II; ESA Biosciences, Inc., MA, USA) according to running conditions reported previously (Umemura *et al.*, 2006).

Hepatic TBARS levels were determined in six liver samples from each group using the method of Ohkawa *et al.* (1979). Briefly, 0.2 ml of liver homogenate was mixed with 1.15% KCl (18 mg/ml protein), 0.2 ml of 8.1% sodium dodecyl sulfate and 3.0 ml of 0.4% thiobarbituric acid in 10% acetic acid (pH 3.5), heated at 95°C for 60 min and then cooled. The reaction mixture was centrifuged at 4,000 rpm for 10 min after 1.0 ml of distilled water and 5.0 ml *n*-butanol and pyridine (15:1, v/v) were added. The absorbance of the resulting solution was determined spectrophotometrically at 532 nm using the Synergy HT Multi-Detection Microplate Reader (BioTek). The levels of TBARS were expressed as the equivalents of the malondialdehyde (MDA) amounts that were produced from 1,1,3,3-tetramethoxypropane.

Statistical analysis

All data are expressed as means with their standard deviations. Multigroups (Control, DEN-alone, DEN-Low ORPH and DEN-High ORPH groups) were used to test the homogeneity of variance between the groups by Bartlett's test. When the data were homogenous, Tukey's test was used, and when heterogeneous, Steel-Dwass test was used. A P value of less than 0.05 was considered statistically significant.

RESULTS

Body and liver weights, food and water consumption and estimated compound intake

During the experimental period, no clinical symptoms or deaths that might be related to the treatment were observed in either of the ORPH-treated groups. Body weight gains during the treatment period were significantly lower in the DEN-ORPH groups than in the control and DEN-alone groups (Fig. 1). Food consumption and water intake were significantly lower in the DEN-High ORPH group than in the control group (Table 2).

At necropsy, body weight was decreased dose-dependently by ORPH treatment. There were no significant differences in the absolute liver weights among the groups. Relative liver weights were significantly higher in the DEN-ORPH treated groups compared with the control and DEN-alone groups. The estimated daily intakes of ORPH in the DEN-Low ORPH and DEN-High ORPH groups calculated from total intakes were 40.4 and 73.9

Table 2. Body weight, food, and liver weight of rats given ORPH for 6 weeks after DEN initiation

Groups	control	DEN-alone	DEN-Low ORPH	DEN-High ORPH
Number of rats	7	11	11	12
Final body weight (g)	264.6 ± 12.3[a]	256.1 ± 12.2	245.1 ± 14.8*	210.3 ± 10.9**,##
Food intake (g/rat/day)[b]	13.0 ± 1.4	11.4 ± 0.7	11.9 ± 0.3	10.2 ± 0.1**
Total ORPH intake (mg/kg BW)			1805.0	3327.7
Water intake (g/rat/day)[b]	18.2 ± 1.4	18.0 ± 0.2	17.5 ± 0.8	13.2 ± 1.9*,##
Absolute liver weight (g)	7.1 ± 1.4	7.8 ± 0.8	8.0 ± 0.6	8.3 ± 0.6
Relative liver weight (% BW)	2.7 ± 0.5	3.0 ± 0.2	3.3 ± 0.1*,#	3.9 ± 0.2**,##

BW: Body weight.

[a]: Values are expressed as mean ± S.D.

[b]: Calculated from the last monitoring data.

*: $p < 0.05$, **: $p < 0.01$ significantly different from the control group (Tukey's test).

#: $p < 0.05$, ##: $p < 0.01$ significantly different from the DEN-alone group (Tukey's test).

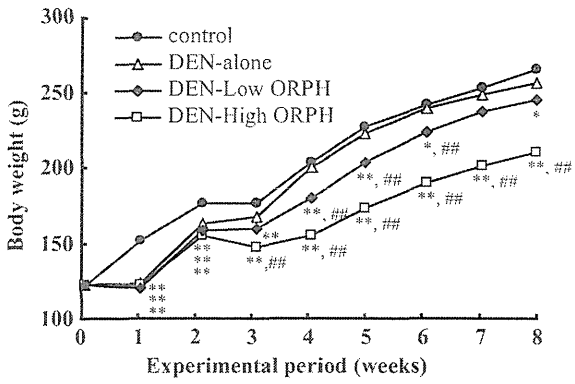

Fig. 1. Body weights of hepatectomized rats in control (black circles), DEN-alone (white triangles), DEN-Low ORPH (black diamonds), and DEN-High ORPH (white squares) groups. * $p < 0.05$, ** $p < 0.01$ significantly different from the control group (Tukey's test). ## $p < 0.01$ significantly different from the DEN-alone group (Tukey's test).

mg/kg body weight/day, respectively (Table 2), and these values were almost equal to the expected intake in the study.

Histopathological examinations

Histopathological examination of the liver samples showed centrilobular hepatocyte hypertrophy with eosinophilic cytoplasm and diffuse vacuolar degeneration in the ORPH treated groups (Fig. 2). Eosinophilic hepatocellular altered foci were also observed in the DEN-alone group and all of the ORPH treated groups.

GST-P positive foci, cell proliferation, and CAR protein expression in the liver

ORPH treatment significantly increased both the number and area of GST-P positive foci compared with the control and DEN-alone groups (Figs. 2 and 3). The PCNA-positive ratio was significantly higher in the DEN-ORPH groups compared with the control group (Figs. 2 and 3). Additionally, CAR was more clearly localized in the nuclei of liver cells in the DEN-ORPH groups compared with the DEN-alone group (Fig. 2).

cDNA microarray and real-time RT-PCR analyses

Hepatic gene expression changes were screened in one rat from each of the groups using an oligonucleotide microarray. In the CodeLink Bioarray, the expression of 392 genes showed a more than two-fold increase while 205 genes were decreased by more than a half in the rat of the DEN-High ORPH group as compared with the rat of the DEN-alone group (Supplemental data). Among the upregulated genes, we focused on the phase I drug-metabolizing enzymes, oxidative stress response-related genes, and CAR-related genes. Real-time RT-PCR analysis was performed on the genes listed in Table 1 in the livers of six rats per group (Table 3). Among the phase I drug-metabolizing enzymes, a significant increase was observed in the gene expression of *Cyp1a1* in the DEN-High ORPH rats and of *Cyp2b1/2* in all DEN-ORPH treated rats compared with the DEN-alone group. Furthermore, antioxidant and/or detoxifying genes against oxidative stress such as *Gpx2* and *Gstm3* were significantly higher in the DEN-High ORPH group compared with the DEN-alone group. In addition, the mRNA level of *Mrp2*, a CAR related-gene, was significantly high-